King's Research Portal

[Link to publication record in King's Research Portal](#)

Accepted Manuscript

Relation between clinical risk factors, early cortical changes, and neurodevelopmental outcome in preterm infants

Karina J. Kersbergen, François Leroy, Ivana Išgum, Floris Groenendaal, Linda S. de Vries, Nathalie H.P. Claessens, Ingrid C. van Haastert, Pim Moeskops, Clara Fischer, Jean-François Mangin, Max A. Viergever, Jessica Dubois, Manon J.N.L. Benders
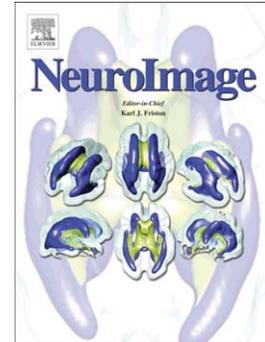
Please cite this article as: Kersbergen, Karina J., Leroy, François, Išgum, Ivana, Groenendaal, Floris, de Vries, Linda S., Claessens, Nathalie H.P., van Haastert, Ingrid C., Moeskops, Pim, Fischer, Clara, Mangin, Jean-François, Viergever, Max A., Dubois, Jessica, Benders, Manon J.N.L., Relation between clinical risk factors, early cortical changes, and neurodevelopmental outcome in preterm infants, *NeuroImage* (2016), doi: 10.1016/j.neuroimage.2016.07.010

Relation between clinical risk factors, early cortical changes, and neurodevelopmental outcome in preterm infants

Karina J. Kersbergen[a], François Leroy[b], Ivana Išgum[c], Floris Groenendaal[a], Linda S. de Vries[a], Nathalie H.P. Claessens[a], Ingrid C. van Haastert[a], Pim Moeskops[c], Clara Fischer[d], Jean-François Mangin[d], Max A. Viergever[c], Jessica Dubois[b], Manon J.N.L. Benders[a,e]

[a]Department of Neonatology, Wilhelmina Children's Hospital and Brain Center Rudolf Magnus, University Medical Center Utrecht, Utrecht, The Netherlands.

[b]INSERM, Cognitive Neuroimaging Unit U992; CEA, Neurospin Center, Saclay, France; University Paris Sud, Orsay, France.

[c]Image Sciences Institute, University Medical Center Utrecht, Utrecht, The Netherlands.

[d]CEA, UNATI, NeuroSpin, Saclay, France.

[e]Centre for the Developing Brain, Division of Imaging Sciences and Biomedical Engineering, King's College London, London, United Kingdom.

Corresponding author:

M.J.N.L. Benders, MD PhD

University Medical Center Utrecht

Department of Neonatology; KE 04.123.1

P.O. box 85090

3508 AB Utrecht

The Netherlands

Tel: 0031- (0)88 755 54545

Email: m.benders@umcutrecht.nl

Running title: Early cortical folding in preterm infants

Abstract

Cortical folding mainly takes place in the third trimester of pregnancy and may therefore be influenced by preterm birth. The aim of this study was to evaluate the development of specific cortical structures between early age (around 30 weeks postmenstrual age) and term-equivalent age (TEA, around 40 weeks postmenstrual age) in 71 extremely preterm infants, and to associate this to clinical characteristics and neurodevelopmental outcome at two years of age. First, analysis showed that the central sulcus (CS), lateral fissure (LF) and insula (INS) were present at early MRI in all infants, whereas the other sulci (post-central sulcus [PCS], superior temporal sulcus [STS], superior [SFS] and inferior [IFS] frontal sulcus) were only seen in part of the infants. Relative growth from early to TEA examination was largest in the SFS. A rightward asymmetry of the surface area was seen in development between both examinations except for the LF, which showed a leftward asymmetry at both time points. Second, lower birth weight z-score, multiple pregnancy and prolonged mechanical ventilation showed negative effects on cortical folding of the CS, LF, INS, STS and PCS, mainly on the first examination, suggesting that sulci developing the earliest were the most affected by clinical factors. Finally, in this cohort, a clear association between cortical folding and neurodevelopmental outcome at two years corrected age was found, particularly for receptive language.

2

Abbreviations

BSITD-III	Bayley Scales of Infant and Toddler Development, third edition
BWZ	Birth weight z-score
CS	Central sulcus
cUS	Cranial ultrasound
IFS	Inferior frontal sulcus
INS	Insula
IVH	Intraventricular haemorrhage
LF	Lateral fissure
MRI	Magnetic resonance imaging
PCS	Postcentral sulcus
PHVD	Post-haemorrhagic ventricular dilatation
PMA	Postmenstrual age
SFS	Superior frontal sulcus
STS	Superior temporal sulcus
TE	Echo time
TEA	Term equivalent age
TR	Repetition time

1. Introduction

During the third trimester of pregnancy, large morphological changes occur in the human brain. Not only an impressive volumetric growth, but also the majority of cortical gyrification and sulcation takes place during this period of brain development, changing the human brain from its largely lissencephalic appearance at 24 weeks of gestation to a brain folded similarly to an adult brain at term age (Habas *et al.* 2012; Clouchoux *et al.* 2012; Battin *et al.* 1998; Chi *et al.* 1977). Many different mechanisms to explain cortical folding have been proposed, but no clear consensus has been reached so far. Two of the most popular theories are the tension-based theory, which states that tension along growing axons causes folding (Van Essen, 1997), and the differential growth hypothesis, which states that folding is driven by different growth rates between various regions and layers of the brain (Xu *et al.* 2010; Toro and Burnod 2005). A recent study integrated both theories and proposed a morphogenetic model based on a growing outer surface and a stretch-driven growing inner core (Budday *et al.* 2014). This model showed good prediction of cortical folding between 27 and 32 weeks of gestation. A similar theory has been described looking at cortices of several mammalian species (Tallinen *et al.* 2014).

Over the last decades, magnetic resonance imaging (MRI) has been used to visualize these changes *in vivo*, and to describe the standard order in which sulci develop (Dubois *et al.* 2008b; Garel *et al.* 2001; van der Knaap *et al.* 1996). With foetal MR imaging normal development has been studied, although it still has its methodological challenges mainly related to motion of the infant and maternal womb/rib cage, as well as constraints in acquisition time. Studies using foetal MRI have shown the characteristic pattern of folding, with primary folds actively developing from 25 weeks onwards, and secondary folds starting to delineate after 30 weeks (Clouchoux *et al.* 2012; Garel *et al.* 2001; Habas *et al.* 2012). Studies of preterm infants imaged *ex utero* have also detailed the progression of folding

4

(Dubois *et al.* 2008b). Some discrepancies between folding patterns measured at birth and those measured in utero at equivalent ages have been described (Lefevre *et al.* 2015). Infants born extremely preterm spend the last trimester of gestation outside the womb, in a neonatal intensive care environment in which they are exposed to a multitude of potentially damaging factors. This may lead to disturbances in the normal folding process taking place during this critical period for brain development (Ajayi-Obe *et al.* 2000; Dubois *et al.* 2008b; Lefevre *et al.* 2015), which may be reflected in impaired neurodevelopmental outcome of especially the cognitive and behavioural domains that are frequently seen in this population (Kapellou *et al.* 2006; Rathbone *et al.* 2011). So far, studies evaluating cortical folding in preterm infants up to term equivalent age (TEA) have been mainly cross-sectional, and longitudinal relationships with neurodevelopmental outcome have remained scarce. Measurements were further applied to the entire brain or to large brain regions involved in several functional networks (Dubois *et al.* 2008b; Kapellou *et al.* 2006; Melbourne *et al.* 2014).

Thus, the aim of this study was to evaluate folding of specific sulci in a longitudinally scanned cohort of extremely preterm infants, and to correlate this with both clinical characteristics and neurodevelopmental outcome at two years of age.

5

2. Materials and methods

2.1 Clinical data

Between June 2008 and March 2013, preterm infants with a gestational age at birth between 24 and 28 weeks, admitted to the level three neonatal intensive care unit of the Wilhelmina Children's Hospital/University Medical Center Utrecht, were consecutively included in a prospective neuroimaging study. Permission from the medical ethics review committee was obtained for this study. Infants were scanned twice: once –if clinically stable- around 30 weeks postmenstrual age (28.7-32.7 weeks) and again around TEA (40.0-42.7 weeks). Serial imaging data were acquired in 137 of the 265 infants born during the inclusion period. Most of the infants that were not scanned serially either died (n=32), were too unstable to be transported to the MRI scanner (n=62), or their parents did not give permission for the MRI (n=17). Forty-three of the 137 serially scanned infants were not yet two years of corrected age at the time of this report, and their outcome data were therefore not yet available. Of the remaining 94 infants, severe motion artefacts on either of the scans was reason for exclusion in 10 infants and in an additional 13 infants, segmentation errors were too severe to correctly process the data, leading to a final cohort of 71 infants to be included in this study. *Supplementary fig. 1* shows a flowchart with the final inclusion of all infants. Perinatal data were obtained by chart review. Birth weight z-scores (BWZ) were computed according to the Dutch Perinatal registry reference data (Visser *et al.* 2009). Corrected weight at scan was defined based on the z-score of the absolute weight at scan, thus correcting for the intrinsic differences between boys and girls. Socioeconomic status was determined based on maternal educational level (Divisie Sociale en ruimtelijke statistieken, 2014). Prolonged mechanical ventilation was defined as total duration of mechanical ventilation before the first scan of >7 days and this parameter was used as a measurement of severity of illness. Serial cranial ultrasound (cUS) was obtained and reported as part of standard clinical care. Intraventricular

haemorrhage (IVH) grading on cUS was scored according to Papile and post-haemorrhagic ventricular dilatation (PHVD) was defined as a ventricular index 4 mm > 97th percentile (Papile *et al.* 1978; Levene, 1981).

2.2 MRI acquisition

MR imaging was performed on a 3.0 tesla MR system (Achieva, Philips Medical Systems, Best, The Netherlands). At the early MRI, infants were scanned in an MRI compatible incubator (Dräger MR Incubator, Lübeck, Germany and later Nomag® IC 3.0, Lammers Medical Technology GmbH, Lübeck, Germany, with a dedicated neonatal head coil), while at TEA an 8-channel SENSE (sensitivity encoding) head coil was used. The protocol included T2-weighted imaging with a turbo spin echo sequence in the coronal plane (at early MRI: repetition time [TR] 10085 ms; echo time [TE]120 ms; slice thickness 2 mm, in-plane spatial resolution 0.35x0.35 mm; at TEA: TR 4847 ms; TE 150 ms; slice thickness 1.2 mm, in-plane spatial resolution 0.35x0.35 mm). After evaluation by a paediatric radiologist, all scans were re-assessed by two neonatologists (LdV and MB) with over 10 years of experience in neonatal neuro-imaging. The presence of IVH, periventricular haemorrhagic infarction, PHVD, cystic periventricular leukomalacia, punctate white matter lesions, central or cortical grey matter infarctions and punctate or larger lesions in the cerebellum were noted.

2.3 MR image post-processing

In order to assess the folding stage and measure changes in cortical sulci, a dedicated approach was implemented by taking benefit of the complementarity of three previously validated methods that enable 1) reliable brain tissue segmentation of preterm images (Moeskops *et al.* 2015), 2) relevant 3D reconstructions of inner cortical surfaces in infants (Leroy *et al.* 2011), and 3) sulci identification in the adult brain (Fischer *et al.* 2012). First, T2-weighted images were segmented with a recently developed automatic segmentation method, defining masks of the cortical grey matter, unmyelinated white matter and

cerebrospinal fluid in the extracerebral space (Moeskops *et al.* 2015). In short, this method

uses supervised voxel classification on T2-weighted images in three subsequent stages. In the

first stage, voxels that can be easily assigned to one of the three tissue types are labelled. In

the second stage, dedicated analysis of the remaining voxels is performed. The third stage is

used to resolve possible inconsistencies resulting from the first to tissue-specific segmentation

stages by performing multi-class classification (Moeskops *et al.* 2015). Before the

segmentation, a brain mask was automatically generated based on the T2-weighted image

using the Brain Extraction Tool (BET) from the FMRIB Software Library (FSL) (Smith,

2002). For both early and TEA segmentations, the same set of features was used.

This method has been evaluated on images of preterm infants acquired at both early and term

equivalent age, and has been validated by comparison with several manually segmented

scans, as described in detail in (Moeskops *et al.* 2015). Because the third stage from

Moeskops' timeline was not yet fully implemented at the time we started to analyse the data,

segmentations resulting from the second stage were used to subsequently reconstruct inner

cortical surfaces of both hemispheres, by adapting the anatomical pipelines of the

BrainvVISA® software (Baby and Morphologist pipelines) (Leroy *et al.* 2011; Mangin *et al.*

2004). Probability maps for the tissues of interest (cortical grey matter, unmyelinated white

matter and cerebrospinal fluid) (Moeskops *et al.* 2015) were combined within a single feature

map to maximize the contrast between grey and white matter. This optimized feature field

was used in the stage of homotopic deformation of coupled surfaces (Leroy *et al.* 2011),

which computes a mask of white matter with homotopic properties and reconstructs 3D

meshes of inner cortical surfaces. While this method is already robust to partial volume

effects and loss of tissue contrast due to maturation up to six months after birth (Leroy *et al.*

2011), we further increased its performance by using probability maps as an extra feature.

Where necessary, the resulting automatic segmentations and meshes were manually corrected

to obtain biologically relevant surfaces. Corrections were performed by two of the authors (KJK and NHPC), with one author (KJK) judging all the final segmentations and meshes. For these corrections the result of the automatic segmentation, the cortex mesh and the MR image with maximum tissue contrast were compared. Errors were detected onto the 3D mesh, carefully checked using the MR image and corrected in the segmentation image using the software editing tool. Training sessions with both authors took place to secure correction was done the same way, and repartition of segmentations was done in a random way, preventing systematic bias. Segmentation correction occurred during a relatively short period, which prevents risk of significant drift in segmentation rating.

From the final meshes, sulcal objects were automatically detected in the places where folding was sufficiently pronounced (i.e. no sulci was identified at the level of small dimples) (Fischer *et al.* 2012). The sulci labels were recognized by means of statistical probabilistic anatomy map modelling (SPAM), implemented for the adult brain (Perrot *et al.* 2011). The accuracy of sulcal labelling was checked visually and, if necessary, adjusted for the sulci of interest in each hemisphere. Left and right hemispheres, as well as early and TEA scans of each infant, were inspected together to provide intra-subject consistency of the sulci labelling across hemispheres and ages. Since not all sulci were visible at the first scan, we decided to analyse only those sulci that were visible at the first scan in over 50% of the infants. Additionally, owing to the difficulty to accurately segment the medial part of the brain in particular in the occipital region, only sulci of the lateral surface were taken into account. Our sulci of interest were thus the following: central sulcus (CS), lateral fissure (LF), insula (INS), superior temporal sulcus (STS), postcentral sulcus (PCS), superior (SFS) and inferior (IFS) frontal sulcus. Since the pre-central sulcus has been shown to develop from the posterior parts of the SFS and IFS and its spatial extent is therefore hard to delineate at the early scan (Dubois *et al.* 2008b), its ventral and dorsal parts were studied at both time points together

with the IFS and SFS, conversely. Only the primary fold of each sulcus was labelled, taking into account the part of the fold that was visible at the early MRI. Secondary and tertiary folds and branches were not considered to make comparison between early and TEA imagingas reliable as possible. An example of selected sulci at both time points is shown in *fig. 1*.

2.4 Computation of parameters characterizing cortical folding

For each sulcus and for both the early and TEA scans, sulcal surface area and mean geodesic depth were extracted using BrainVISA® (Leroy *et al.* 2011; Mangin *et al.* 2004; Fischer *et al.* 2012). For the LF, sulcal length was also computed. For the INS, only surface area was computed, since depth of the INS is not an informative parameter, because the INS as computed with BrainVISA® does not refer to the sulcus but to the whole structure. For the sake of clarity, we will however keep referring to the INS as a sulcus throughout the rest of the paper. Surface areas of each hemisphere hull were computed by the morphological closing of the brain segmentation, as a measure of overall hemisphere size (Fischer *et al.* 2012; Germanaud *et al.* 2012). To correct for inter-individual variability in brain size, a sulcal index was calculated per sulcus by dividing the surface area of the given sulcus by the surface area of the hemisphere hull. Asymmetry indices in surface area and mean depth were calculated for all individual sulci as [sulcus left hemisphere – sulcus right hemisphere]/[sulcus left hemisphere + sulcus right hemisphere]. For the LF, we also investigated whether asymmetry in length, which has been reported in healthy adults (Foundas *et al.* 1999), is already present at these ages. For both surface area and mean depth, the absolute growth per week (in mm^2 and mm, respectively) was calculated in each hemisphere as the difference between the TEA and the early scan measures, divided by the difference in postmenstrual age in weeks (PMA) between both scans. Relative growth per week (in %) was defined as the absolute growth rate per week, divided by the corresponding measure at TEA.

2.5 Assessment of neurodevelopmental outcome

Neurodevelopmental outcome was assessed at either 24 or 30 months' corrected age (i.e. corrected for gestational age at birth), dependent on inclusion in a European study (www.i-med.ac.at/neobrain). Neurodevelopmental assessment was performed by a single developmental specialist (ICH) using the cognitive, fine motor and gross motor subtests of the Bayley Scales of Infant and Toddler Development, third edition (BSITD-III) (Bayley, 2006). In the infants seen at 30 months' corrected age, the expressive and receptive language subtests were also performed. Composite and scaled scores were calculated (mean [standard deviation] in a normative population: 100 [15] and 10 [3], respectively). No difference in scores was found between infants tested at 24 (n=34) and 30 months (n=37) and data of both groups were therefore combined.

2.6 Statistical analyses

Statistical procedures were performed using Matlab (MATLAB and Statistics Toolbox Release 2013b, The MathWorks Inc., Natick, MA, USA) and R (version 2.15.3 www.r-project.org).

Paired samples t-tests were used to compare the left and right surface areas and mean depths for asymmetry, as well as for growth of the sulci between both scans. To assess whether overall brain size in general was of influence, we also computed sulcal indices, defined as surface area divided by overall hemispheric hull area. These indices were used as an additional measurement in the general linear modelling.

General linear modelling was performed to associate brain morphological measures (as dependent variables) with the clinical characteristics of the infants (as independent variables). For each sulcus, absolute surface area, mean depth and sulcal index at early and TEA imaging, and growth of surface area and depth between both scans were studied. All models were corrected for PMA at MRI. For the early and the growth rate models, the infants in

11

which the sulcus was not yet identifiable were excluded. Sex and multiple pregnancy were included as dependent variables in the model based on the literature (Dubois *et al.* 2008b; Dubois *et al.* 2008a; Vasileiadis *et al.* 2009). Since only two infants were small for gestational age (defined as a birth weight below the 10th percentile), BWZ was included instead of small for gestational age. Severe IVH (grade III-IV) was included as a measure for brain injury and prolonged mechanical ventilation (>7 days) was chosen as an overall parameter measuring severity of illness. To assess whether there was an intrinsic effect of sex on cortical folding, not explained by the difference in weight at the time of scanning, general linear modelling was repeated with the interaction between sex and corrected weight at scan in the model instead of BWZ. Besides significance, we also display effect sizes in the results for all significant parameters. Effect size (E) is depicted as percentage and was calculated as the percentage of the estimate from the clinical variable compared to the intercept.

Next, we evaluated whether outcome parameters around two years of age might be explained by cortical folding measures in the neonatal period. General linear modelling was performed to correlate outcome parameters (as dependent variables) and morphological measures (as independent variables: absolute surface area, mean depth and sulcal index at early and TEA imaging, and growth between both scans for each sulcus). In these analyses, all data were corrected for PMA, socio-economic status and sex. For the gross motor subscale, the CS, SFS and IFS were considered, since the pre-central sulcus was included in both the SFS and the IFS. For the fine motor subscale, the PCS was added to the CS, SFS and IFS because of the possible role of the parietal lobe on praxia. For the cognitive subscale all sulci were taken into account (one after the other), because we had no hypothesis on specific brain regions to be involved in cognitive development. Since peri-sylvian regions are activated before term equivalent age by speech perception in preterm born infants (Mahmoudzadeh *et al.* 2013), the LF, INS, STS and IFS were tested for the language subscales. To correct for the multiple sulci

12

that were assessed, a p-value ≤ 0.007 (0.05/7 sulci) was considered significant in the

multivariable analyses.

3. Results

Clinical characteristics, MRI parameters and outcome data of all infants are summarized in *table 1*. Mean gestational age at birth was 26.5 weeks, mean PMA at the early scan 30.7 weeks and at the term equivalent scan 41.2 weeks.

Clinical characteristics	Mean (range) or N (percentage)
Gestational age at birth (weeks)	26.5 (24.4 – 27.9)
Birth weight (grams)	903 (460 – 1350)
Birth weight z-score	0.4 (-2.5 – 1.8)
Sex (male/female)	36/35 (51/49%)
Multiple pregnancy (single/multiple)	49/22 (69/31%)
Small for gestational age	2 (3%)
>7 days of mechanical ventilation	25 (35%)
Patent ductus arteriosus requiring treatment	35 (49%)
Chronic lung disease	20 (28%)
Culture proven sepsis	25 (35%)
Necrotizing enterocolitis requiring surgery	7 (10%)
IVH (0/1/2/3/4)	44/8/11/5/3 (62/11/15/7/4%)
PHVD +4mm > 97th centile	7 (10%)
Postmenstrual age at early MRI (weeks)	30.7 (28.7 – 32.7)
Week of post-natal life at early MRI (weeks)	4.1 (0.9-8.1)
Weight at early MRI (grams)	1205 (620-1785)
Postmenstrual age at TEA MRI (weeks)	41.2 (40.0 – 42.7)
Week of post-natal life at TEA MRI (weeks)	14.7 (12.3-17.1)
Weight at TEA MRI (grams)	3326 (2045 – 4315)

Follow-up

Maternal education (low/middle/high)	19/24/28 (27/34/39%)
Corrected age at follow-up (months)	27.2 (23.2 – 30.8)
Subgroup seen at 24 months (n=35)	24.2 (23.2-27.0)
Subgroup seen at 30 months (n=36)	30.1 (29.5-30.8)
Gross motor scaled score	10 (3 – 17)
Fine motor scaled score	13 (9 – 19)
Total motor composite score	109 (79 – 148)
Cognitive composite score	104 (85 – 130)
Expressive language scaled score (N=34)	12 (7 – 17)
Receptive language scaled score (N=35)	11 (8 – 16)
Total language composite score (N=34)	110 (89 – 135)

Table 1: Baseline characteristics (N=71)

3.1 Progression of cortical folding

At the early scan, the CS, LF and INS were present in all infants. For the other sulci, the presence at the first scan differed, as can be seen in *table 2*. Of those sulci, the STS was most often present, followed by the IFS, PCS and SFS. When a sulcus was only present on one side, this occurred more often in the right than the left hemisphere, as shown in *table 2*. As shown in the graphs in *fig. 1* and also in the examples in *fig. 2*, large inter-individual differences were seen between infants scanned at the same PMA, with a wider variation in surface area at TEA compared with early imaging.
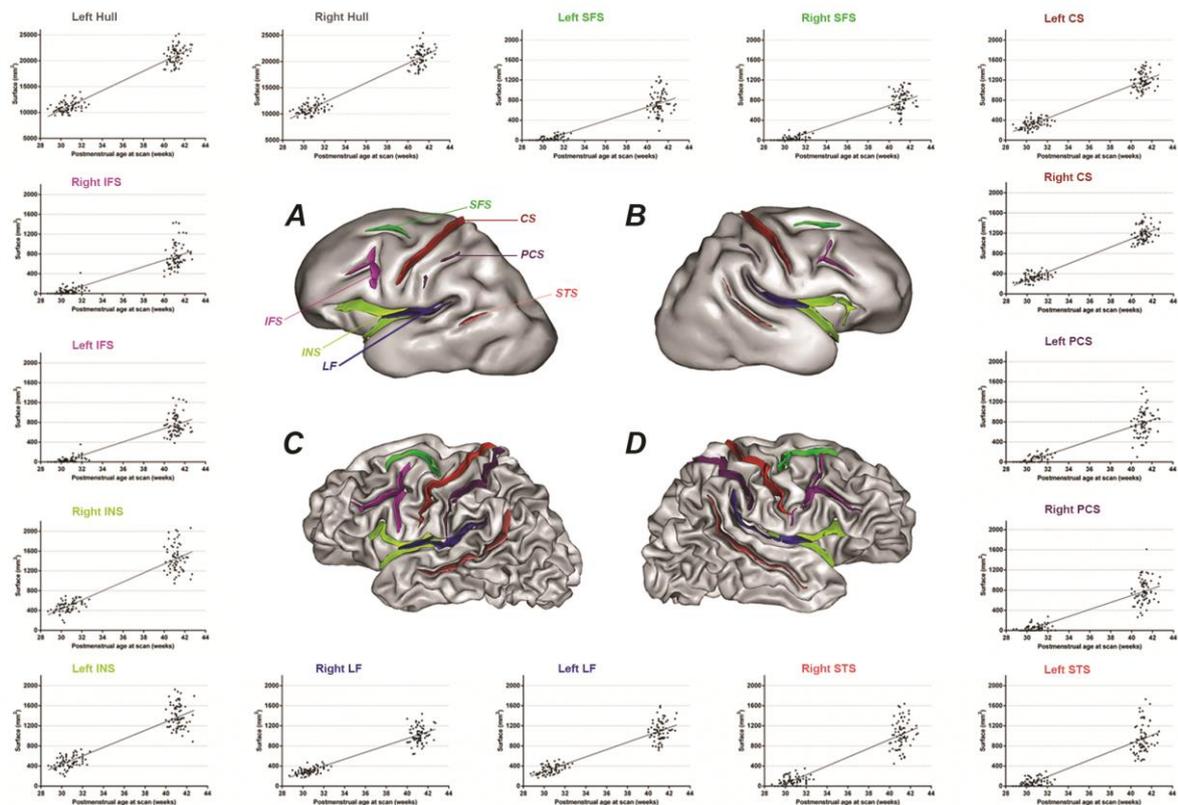
Figure 1 Longitudinal development of sulci

Examples of inner cortical surfaces showing the selected sulci in a single infant. Meshes from the left (A, C) and right (B, D) hemispheres are shown at early (top) and TEA imaging (bottom). The following colours represent the sulci: red – central sulcus (CS); blue – lateral fissure (LF); light green – insula (INS); vale pink – superior temporal sulcus (STS); purple – postcentral sulcus (PCS); green – superior frontal sulcus (SFS); pink – inferior frontal sulcus (IFS). Around these examples, graphs are depicted showing the absolute surface areas of each sulcus, both left and right, at early and TEA imaging for all infants as a function of PMA at scan. Note the large inter-individual variability in surface areas at TEA for all sulci, independent of age at MRI, whereas at the early scan, areas show increases with an increasing age at MRI.

16
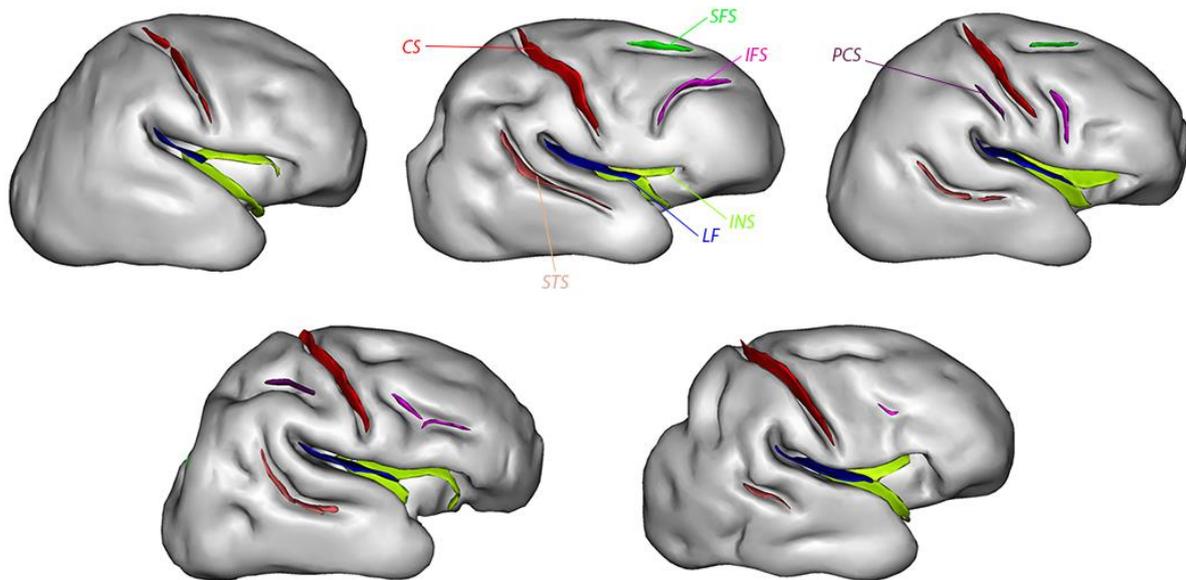
Figure 2 Inter-individual variability in folding progression at early MRI

Meshes of the right hemispheres from five different infants, all scanned at 29.86 weeks PMA.

Note the differences in the number of sulci present between the infants, as well as in their

localization and shapes, especially for frontal sulci. The same colour representation and

abbreviations as in Fig. 1 are used.

Sulcus	Presence			
	Both sides	**Only right side**	**Only left side**	**Neither side**
Central sulcus	71 (100%)	-	-	-
Lateral fissure	71 (100%)	-	-	-
Insula	71 (100%)	-	-	-
Superior temporal sulcus	54 (77%)	5 (7%)	5 (7%)	7 (10%)
Inferior frontal sulcus	34 (48%)	16 (23%)	7 (10%)	14 (20%)
Postcentral sulcus	28 (39%)	12 (17%)	7 (10%)	24 (34%)
Superior frontal sulcus	27 (38%)	11 (15%)	4 (6%)	29 (41%)

Table 2: Presence of sulci at early scan (N=71)

At the early scans, morphological measures (surface area and depth, and sulcal index) seemed to correlate strongly with PMA for all sulci, whereas at TEA these correlations were no longer visible (*fig. 1*).

All sulci showed a clear growth between both scans, both in surface area (*fig. 1*) and in mean geodesic depth. Absolute and relative growth rates are shown in *fig. 3*. All studied sulci increased in size, at a rate of about 10% as compared with the increase in overall brain size. The relative growth of the sulci (i.e. after normalizing by their size at TEA scan), was larger than the relative growth of the overall brain. The SFS showed the largest relative growth, followed by the PCS, IFS and STS. The three sulci that developed first (CS, LF and INS, which were present on all early scans) showed a relative smaller growth, although absolute growth was large in these sulci.
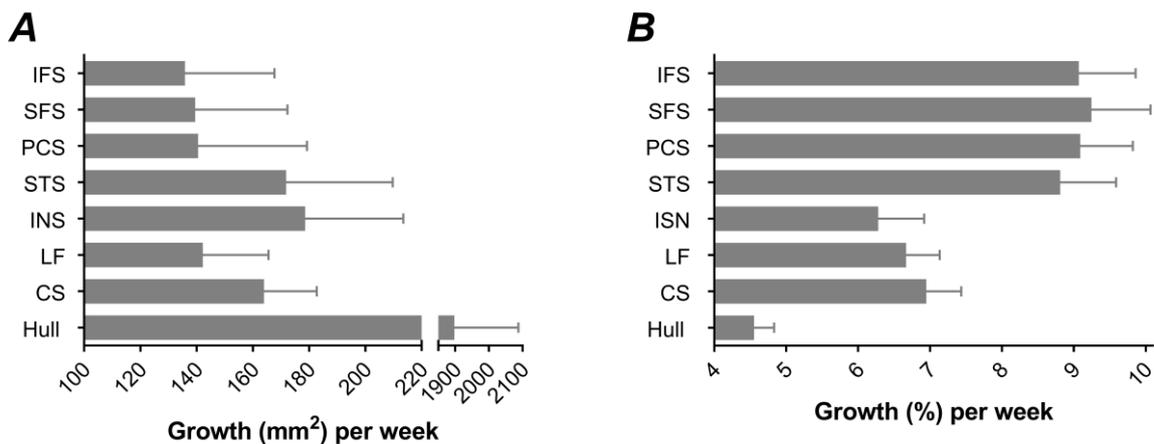

Figure 3 Sulcal growth

This figure shows the absolute and relative growth of the sulci. Growth is represented as either absolute surface increase per week (A, in mm^2) or relative surface increase per week (B, in %), compared with the surface at TEA.

3.2 Sulcal asymmetries

Mean asymmetry indices between left and right hemispheres and standard deviations are represented in *fig. 4* for all sulci. Significant inter-hemispheric differences in surface area and depth were found for the following sulci. CS: depth at early scan, rightward direction; LF: surface area and sulcal length at both time points, leftward asymmetry with additionally also LF depth at TEA; INS: surface area at TEA, rightward direction; STS: surface area and depth at both early and TEA,rightward direction; SFS: depth at TEA, rightward direction; IFS: surface area at early scan, depth at both early and TEA scans, rightward direction.). Note that although significant, asymmetry indices were below the 5% threshold that is often used to describe asymmetry (Galaburda *et al.* 1987), for the LF (surface area and length at early MRI, surface area at TEA), and the INS (surface area at TEA).
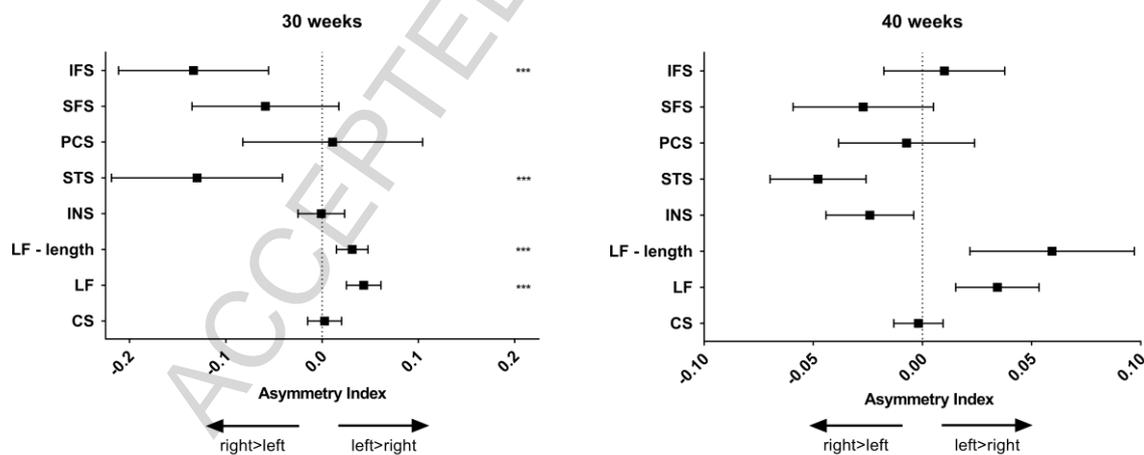
Figure 4 Sulcal asymmetries

The asymmetry indices of the surface areas of all sulci, and of the sulcal length of the lateral fissure are represented in this figure for the early (A) and TEA (B) scans. The square represents the mean value, with the whiskers extending to the 95% confidence interval. Significant differences are indicated as follows: <0.05 '', <0.01 '**', <0.001 '***'.*

3.3 Clinical characteristics influencing cortical folding

Fig. 5 shows the schematic results of the multivariable analyses comparing morphometric parameters at early and TEA scan, and absolute growth with clinical characteristics. Detailed results, including all the statistical measures, are also summarized in *Suppl. table 1*. No significant correlation was found for any sulcal index (surface area divided by overall hemispheric hull area).

When assessing overall brain size (i.e. bilateral hull surface area) at the early scan, we found a positive effect of BWZ and high grade IVH, and a negative effect of prolonged mechanical ventilation. At TEA, the effects of BWZ and prolonged ventilation persisted. Overall brain growth was influenced positively by BWZ and high grade IVH, and negatively by multiple pregnancy and prolonged ventilation for the left hemisphere, but no significant influences were found for the right hemisphere.

In the next paragraphs, the results of *fig. 5* are summarized by clinical characteristic rather than by sulcus, to highlight the reproducible significant effects. First, maternal education did not have a direct effect on the morphological measures for any sulcus.

Second, a higher BWZ had a positive influence on surface area of the bilateral LF and INS at early MRI. At TEA, this effect was observed for the surface area of the left INS and bilateral CS, and for depth of the left STS. BWZ had a positive effect on absolute growth of right CS surface area and depth.

Third, no significant effects of sex were found in the multivariable model for any sulcus. To further assess an intrinsic effect of sex on cortical folding, not explained by a difference in weight, another multivariable model was tested which included weight at MRI corrected for PMA and sex, as well as sex and the interaction between both parameters (BWZ was not considered in this model). Using this model, the left STS and right IFS of boys showed an initially lower surface area at early MRI compared with girls, with a steeper growth and a

larger surface area at TEA (p=0.01 for all analyses). For the left PCS, the surface area of boys was already larger at early MRI and growth was slightly steeper (p=0.02), leading to a larger surface area at TEA (p=0.04). For the left LF, this effect was seen for growth (p=0.02), but no significant differences were found at TEA. To summarise, we observed that some sulci showed larger surface area or growth in boys compared with girls with similar weight. However, none of these differences did persist following correction for multiple comparisons.

Fourth, infants from a multiple pregnancy showed smaller INS surfaces compared with singletons on both sides at early MRI and on the left at TEA, and a smaller depth of the left STS at both ages.

Fifth, infants requiring prolonged mechanical ventilation had smaller surface areas at early MRI of the bilateral LF and INS, as well as a smaller depth of the right CS. At TEA, these effects were no longer found, but the right STS surface area and left PCS depth were lower in infants that required prolonged ventilation. Absolute growth of the left PCS surface area was also negatively influenced by prolonged ventilation.

Sixth, ten infants had a grade III-IV IVH. Presence at early MRI of the STS, PCS, SFS and IFS was lower in these infants compared with the 61 infants without severe IVH. Indeed, in infants with severe IVH, sulcal absence was about two times higher for the bilateral STS, IFS, left PCS and right SFS, and a third higher for the left SFS. Only the right PCS was more frequently present in infants with severe IVH (70%) than in those without (54%). None of these differences were however significant, and the effect of high grade IVH did not reach significance in the multivariable models of sulci folding measurements. Taking the side of the IVH into account did not yield significant differences either.
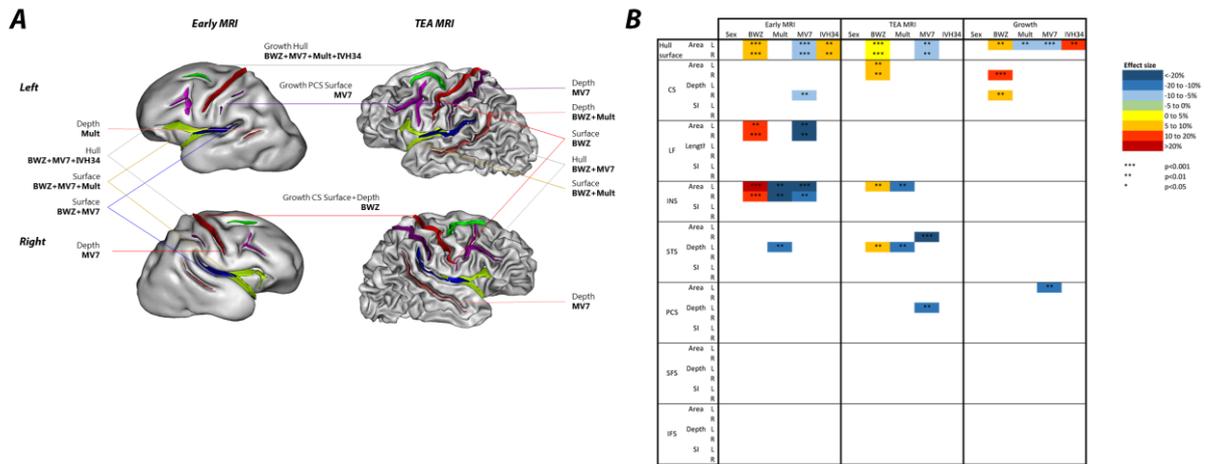
Figure 5 Graphical depiction of clinical risk factors

Findings of the multivariable analyses regarding the clinical risk factors are summarized both graphically (A) and with regards to effect size (B). A: Early (left), and TEA (right) MRI, with growth in between. For each sulcus, clinical characteristics significantly influencing surface area or depth are shown. B: Heatmap depicting the effect sizes for the significant associations. Additional abbreviations: BWZ= birth weight z-score, IVH34= intraventricular haemorrhage grade III-IV, Mult = multiple pregnancy, MV7= mechanical ventilation >7 days.

3.4 Relationships between cortical folding and neurodevelopmental outcome

The relations between outcome during toddlerhood (at 24-30 months) and cortical folding during the neonatal period (around 30 and 40 weeks PMA) were tested per subscale of the BSITD-III. *Fig. 6* shows a schematic summary of all results from the multivariable analyses, while detailed results are presented in *Suppl. table 2*.

No significant correlations between gross and fine motor or cognitive outcome and brain sizeor sulcal indices were found. Gross motor outcome depended on early development of the IFS (bilateral surface area , right depth and left sulcal index) and the depth of the right SFS at early scan. Fine motor outcome was positively correlated with right PCS surface area and right SFS depth at TEA. The cognitive subscale showed a positive correlation with absolute growth of left LF and SFS depth. Although these differences were significant, effect sizes were small for all correlations (≤3%,). Maternal educational level had a significant influence on outcome across all models at both early and TEA MRI (but not for growth), with an effect size between 7 and 18%. Again, sex was not significant in any of these models. When infants with brain injury (IVH grade III-IV) were excluded, only the correlation between cognitive outcome and absolute growth of the left SFS depth remained significant.

In a subgroup of infants, the expressive and receptive language subtests were administered as well. At early MRI, significant correlations between receptive language and folding measures were only observed for the left IFS (surface area and sulcal index). At TEA, effects were found for the bilateral hemispheric size, bilateral LF (surface area, depth and sulcal index), IFS (depth), STS (right: surface area , depth and sulcal index, left: depth) and left INS (surface area, sulcal index). The expressive language subscale correlated with the left IFS at early MRI (surface area) and left LF at TEA (depth). Again, effect sizes were small and the effect of maternal education remained significant in all analyses. When repeating the analyses after exclusion of the infants with brain injury (IVH grade III-IV), all correlations remained

23

significant except the correlation between receptive and expressive language and the left IFS at early MRI.
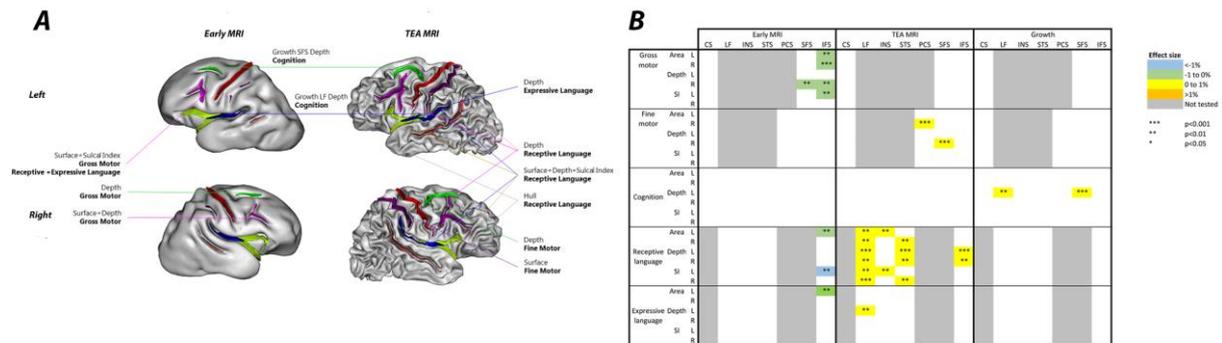
Figure 6 Graphical depiction of neurodevelopmental outcome

Findings of the multivariable analyses regarding neurodevelopmental outcome are summarized both graphically (A) and with regards to effect size (B). A: Early (left) and TEA (right) examinations, with growth in between. For each sulcus is shown whether sulcal surface area, depth or sulcal index had a correlation with the different subscales of neurodevelopmental outcome at 2-2.5 years of age. B: Heatmap depicting the effect sizes for the significant associations.

4. Discussion

This study describes progression of cortical folding during the extra-uterine equivalent of gestation in the third trimester in a cohort of extremely preterm infants with longitudinal MRI. It showed a rightward asymmetry in brain development and regional growth differences. Additionally, the influence of several clinical characteristics and relationship with neurodevelopmental outcome during toddlerhood were studied for specific primary sulci, providing valuable information on the possible deviations related to preterm birth.

4.1 Folding progression and inter-hemispheric asymmetries

Previous post-mortem and in vivo studies of foetuses and preterm newborns have shown that sulcus maturation progresses in a specific order, starting with the central structures (Battin *et al.* 1998; Chi *et al.* 1977; Clouchoux *et al.* 2012; Dubois *et al.* 2008b), progressing to peripheral structures in an occipital to frontal direction (Chi *et al.* 1977; Kersbergen *et al.* 2014; Kinney *et al.* 1988). The current results corroborate those data, as shown by differences in presence or absence of sulci on the early scan. The most central sulci (CS, LF and INS) were present in all infants at the early scan, around 30 weeks PMA. Then folding progressed from the temporal to the frontal and parietal lobes: the STS was seen in 90%, followed by the IFS (80%), PCS (66%) and finally the SFS (59%). These data suggest a slightly later development of the sulci compared with in vivo studies of fetal brain development, where these sulci are shown to develop between 28 and 30 weeks of gestation and thus should be present on the early scan in all infants (Clouchoux *et al.* 2012; Garel *et al.* 2001; Habas *et al.* 2012; Fogliarini *et al.* 2005). Alternatively, this could be attributed to not being able to detect small dimples on the reconstructed cortical surface, owing to image spatial resolution and the analysis technique used to identify sulci (Clouchoux *et al.* 2012; Dubois *et al.* 2008b). There were several limitations of our study that may have influenced our results. First, like in every segmentation method, partial volume effects might have affected tissue segmentations,

especially in the early MRI, where brain sizes was relatively small compared to the image spatial resolution. Nevertheless, this resolution was sufficient to clearly identify the folds visually, in the same way as folds are clearly seen on fetal MRI with thick slices (Girard *et al.* 1995). To partly overcome the bias related to partial voluming, manual corrections were performed. However, we acknowledge that this effect might not be completely balanced between early and TEA examinations. Second, the method for sulci identification also required some manual correction of the segmentations to obtain biologically relevant inner cortical surfaces, particularly at TEA in regions where sulci were very narrow. This was however done in a systematic way. In the future, further advances in image acquisition (e.g. higher field gradients to achieve higher spatial resolution in a reasonable acquisition time) and/or in the post-processing (e.g. use of super-resolution algorithms to reconstruct submillimetric images, improvement of segmentation algorithms) will reduce the need for manual corrections and allow the inclusion of the medial and occipital parts of the brain. Third, we chose not to take secondary and tertiary folds into account at TEA despite the fact that these folds were clearly visible and identified, to make the comparison between early and TEA imaging as clear as possible. Therefore, we cannot comment on the effects of clinical factors on secondary and tertiary folding.

Compared to the sulci that were already well developed at early MRI, relative growth was largest for the sulci that were least developed at early MRI, highlighting the intense folding taking place in the last 10 weeks of pregnancy. These regional differences in growth seem to continue after term birth. Hill and colleagues compared morphology measures of 12 term-born infants with 12 healthy young adults, and also observed regional differences in the degree of expansion, with expansion being twofold higher in the areas of the four sulci we observed to have the most intense folding (STS,PCS, SFS and IFS) (Hill *et al.* 2010b). The higher expanding regions were hypothesized to be less mature at term birth on a cellular level

as well (Hill *et al.* 2010b).

The development of the human brain is known to be asymmetrical, with a slightly earlier development of the right hemisphere compared with the left in terms of cortical folding (Chi *et al.* 1977; Kersbergen *et al.* 2014; Kinney *et al.* 1988). In this study, several inter-hemispheric asymmetries were found. For most sulci (INS, STS, IFS), a rightward asymmetry was appreciated. Only the lateral fissure showed an asymmetry towards the left hemisphere. For the three central sulci (CS, LF, INS) that fold early on, the asymmetry index barely changed between early and TEA imaging. In contrast, the disappearance of rightward asymmetry for IFS, which develops at a later stage, suggests that a delay in left hemisphere development is a likely explanation for the IFS asymmetry, with the left hemisphere catching up with the right by TEA imaging.

The STS rightward asymmetry has been described in many previous studies of brain development before (Chi *et al.* 1977) and has been found in foetuses (Habas *et al.* 2012; Kasprian *et al.* 2011), preterm (Dubois *et al.* 2008b; Dubois *et al.* 2008a) and term born infants (Hill *et al.* 2010a; Li *et al.* 2014; Glasel *et al.* 2011). The STS remains asymmetrical in adults, suggesting an underlying difference in structure rather than a delay in folding to be responsible for this early asymmetry (Van Essen, 2005; Ochiai *et al.* 2004; Leroy *et al.* 2015). The leftward asymmetry of the LF surface area has also been reported before in studies of foetuses, preterm infants and in infancy, mostly focused on the planum temporal (Dubois *et al.* 2010; Glasel *et al.* 2011; Chi *et al.* 1977)(Glasel *et al.* 2011; Hill *et al.* 2010a; Li *et al.* 2014). This asymmetry in LF surface area was partly related to the leftward asymmetry in sulcal length, which increased from early to TEA imaging. Like for the STS, LF asymmetry persists and increases throughout development, as has been shown in a cross-sectional study of children, adolescents and young adults (Sowell *et al.* 2002) and with an earlier study in healthy adults (Foundas *et al.* 1999). Both a deeper right STS and a larger left LF have also

been found in chimpanzees, although weakly (Gannon *et al.* 1998; Hopkins and Nir 2010). These asymmetries in perisylvian regions probably have an old origin in the primate lineage, which would have been amplified in humans by language acquisition which is already predominantly left-sidedin preterm newborns (Mahmoudzadeh *et al.* 2013) and two month old infants (Dehaene-Lambertz *et al.* 2010).

4.2 Inter-individual variability in cortical folding in relation to clinical characteristics

At both scans, inter-individual differences were noted across infants in both size and morphology of the sulci, in agreement with earlier studies, suggesting that besides factors related to preterm birth, genetic factors also partly influence the folding process (Van Essen, 2005; Im *et al.* 2011). The large inter-individual differences and the increase of these variations towards term equivalent age may to some extent cover the effects of clinical risk factors on cortical growth.

Before describing these inter-individual differences, we should point out that our cohort might not be fully representative of all preterm infants. For this study, we focused on those infants with serial imaging, and inclusion may therefore have been biased towards the healthier part of the cohort as the more ill infants were not stable enough to be scanned around 30 weeks PMA. Also, the cohort was not large enough to extensively study clinical risk factors, and interactions between prolonged mechanical ventilation and surgery for example could not be studied.

The CS, LF and INS were most influenced by clinical characteristics. These sulci are all thought to form before 28 weeks gestation (Chi *et al.* 1977; Clouchoux *et al.* 2012). In other words, these sulci are actively folding during the period an extremely preterm infant is most severely ill (i.e. the first weeks ex utero, and possibly also the last weeks in utero, depending on foetal history and cause of preterm birth). Therefore we might assume that developmental

28

disturbances related to preterm birth and severity of illness will have a larger impact on these early developing sulci compared with the later developing sulci whose active folding will occur during a more stable period for most of extremely preterm infants (Wright *et al.* 2014), especially in the absence of severe white matter injury.

Intrauterine growth retardation has previously been described as a risk factor for abnormal cortical folding (Dubois *et al.* 2008a). In the present cohort, only two infants were small for gestational age, which was probably due to a selection bias, as infants born small for gestational age during the inclusion period more often died before admission to the neonatal intensive care unit or were too unstable to receive an early MRI. Proper correlations could therefore not be made. Nevertheless, the effect of BWZ was obvious throughout analyses for most sulci, in agreement with a previous study of preterm infants (Engelhardt *et al.* 2015). Because sulcal indices were not affected by this factor, it suggests that lower sulci surface area and depth related to lower body weight, probably relied on an overall reduction in brain. Lower folding rates of the INS and STS were detected in infants born after multiple pregnancy compared with singletons. An harmonious delay of folding in preterm infants from twin pregnancies has been reported at birth (Dubois *et al.* 2008a) and on autopsy (Chi *et al.* 1977).

The large negative effect of prolonged mechanical ventilation on sulcal measures particularly at early MRI suggests that illness severity in the immediate perinatal period strongly affects cortical folding, in agreement with previous studies (Kaukola *et al.* 2009; Engelhardt *et al.* 2015). At TEA, this effect was less pronounced, suggesting that folding may catch up during the period between both scans. Alternatively, the diminishing effects may be related to the increasing inter-individual variability, as shown in *fig. 1*. Compared with term-born newborns with acute brain injury, the duration of the insult to the white matter is likely to be subacute or chronic in preterm infants. The duration of the insult and the age at onset (e.g. pre- or

postnatal), possibly related to the underlying cause for preterm birth, may influence cortical folding as well. A larger cohort of preterm newborns with extensive antenatal history is needed to study these effects.

Only ten infants in this cohort had a severe IVH (grade III-IV), and these infants seemed to show delayed folding, as suggested by the less frequent presence of STS, PCS, SFS and IFS. This delay may be due to increased intracranial pressure in infants with PHVD in the early stage, or to disturbed connectivity in infants with a periventricular haemorrhagic infarction (Melbourne *et al.* 2014). However, differences were not significant in the multivariable models including all the clinical factors. Other white matter and cerebellar pathologies were sparse in this population and were therefore not taken into account. In a previous study, which included part of the infants of this study, brain injury was related to a decrease of global folding measures and an increase of cortical thickness, which was more pronounced at TEA (Moeskops *et al.* 2013). Further elucidating the effect of the different types of brain injury on cortical folding are required to offer options for evaluating intervention strategies.

4.3 Functional outcome predicted by early cortical folding

Neurodevelopmental outcome measures during toddlerhood were related to folding measures of several sulci during early infancy. Especially many correlations were found for receptive language and folding of perisylvian sulci, as well as for total brain size. This is in agreement with an earlier study of a British population that showed a relation between growth of cortical surface area between 24 and 44 weeks PMA and outcome at two and six years for cognitive functions including language development (Rathbone *et al.* 2011). Furthermore, most correlations remained significant when we considered sulcal indices, thus partly excluding the global effect of total brain size. This results suggest that language development may be predicted not only by brain size, but also by regional differences. Nevertheless, the effect

30

sizes we reported were smaller than those of the British study (Rathbone *et al.* 2011), which could perhaps be explained by the young age at follow-up (2.0-2.5 years) or may be due to the use of different neurodevelopmental tests. In our cohort with a relatively unimpaired outcome at two years of age, outcome at a later age may show a more pronounced effect of early cortical folding on cognitive and language functions. Additionally, the large influence of maternal educational level on neurodevelopmental outcome suggests that both genetic and environmental factors contribute to early development.

In conclusion, this longitudinal MRI study in extremely preterm infants confirmed that cortical folding proceeds asynchronously from the central regions towards the temporal, parietal and frontal lobes, with the right hemisphere developing earlier than the left. By term equivalent age these left-right differences have largely disappeared and only the known asymmetries of the STS and LF were still present, despite larger inter-individual variability in folding measures at TEA compared to early MRI. A lower birth weight z-score, multiple pregnancy and prolonged mechanical ventilation were related to a delay in cortical folding mainly on the early scan, particularly for sulci developing the earliest. A clear correlation between cortical folding and neurodevelopmental outcome at two years was also highlighted. Longer term neurodevelopmental follow-up and a combination of these data with functional imaging are needed to further investigate the effects of preterm birth on brain development.

31

Funding:

References

Ajayi-Obe M, Saeed N, Cowan FM, Rutherford MA, Edwards AD. 2000. Reduced development of cerebral cortex in extremely preterm infants. Lancet. 356: 1162-1163.

Battin MR, Maalouf EF, Counsell SJ, Herlihy AH, Rutherford MA, Azzopardi D *et al*. 1998. Magnetic resonance imaging of the brain in very preterm infants: visualization of the germinal matrix, early myelination, and cortical folding. Pediatrics. 101: 957-962.

Bayley N. Bayley Scales of Infant and Toddler Development, 3rd edition. San Antonio, TX: Harcourt Assessment; 2006.

Budday S, Raybaud C, Kuhl E. 2014. A mechanical model predicts morphological abnormalities in the developing human brain. Sci Rep. 4: 5644.

Chi JG, Dooling EC, Gilles FH. 1977. Gyral development of the human brain. Ann Neurol. 1: 86-93.

Clouchoux C, Kudelski D, Gholipour A, Warfield SK, Viseur S, Bouyssi-Kobar M *et al*. 2012. Quantitative in vivo MRI measurement of cortical development in the fetus. Brain Struct Funct. 217: 127-139.

Dehaene-Lambertz G, Montavont A, Jobert A, Allirol L, Dubois J, Hertz-Pannier L *et al*. 2010. Language or music, mother or Mozart? Structural and environmental influences on infants' language networks. Brain Lang. 114: 53-65.

Divisie Sociale en ruimtelijke statistieken SSt. Standaard Onderwijsindeling 2006; Editie 2013/'14. Den Haag/Heerlen: Centraal Bureau voor de Statistiek; 2014.

Dubois J, Benders M, Borradori-Tolsa C, Cachia A, Lazeyras F, Ha-Vinh LR *et al*. 2008a. Primary cortical folding in the human newborn: an early marker of later functional development. Brain. 131: 2028-2041.

Dubois J, Benders M, Cachia A, Lazeyras F, Ha-Vinh LR, Sizonenko SV *et al*. 2008b. Mapping the early cortical folding process in the preterm newborn brain. Cereb Cortex. 18: 1444-1454.

Dubois J, Benders M, Lazeyras F, Borradori-Tolsa C, Leuchter RH, Mangin JF *et al*. 2010. Structural asymmetries of perisylvian regions in the preterm newborn. Neuroimage. 52: 32-42.

Engelhardt E, Inder TE, Alexopoulos D, Dierker DL, Hill J, Van ED *et al*. 2015. Regional impairments of cortical folding in premature infants. Ann Neurol. 77: 154-162.

Fischer C, Operto G, Laguitton S *et al*. Morphologist 2012: the new morphological pipeline of BrainVISA. 2012.

Fogliarini C, Chaumoitre K, Chapon F, Fernandez C, Levrier O, Figarella-Branger D *et al*. 2005. Assessment of cortical maturation with prenatal MRI. Part I: Normal cortical maturation. Eur Radiol. 15: 1671-1685.

Foundas AL, Faulhaber JR, Kulynych JJ, Browning CA, Weinberger DR. 1999. Hemispheric and sex-linked differences in Sylvian fissure morphology: a quantitative approach using volumetric magnetic resonance imaging. Neuropsychiatry Neuropsychol Behav Neurol. 12: 1-10.

Galaburda AM, Corsiglia J, Rosen GD, Sherman GF. 1987. Planum temporale asymmetry, reappraisal since Geschwind and Levitsky. Neuropsychologia. 25: 853-868.

Gannon PJ, Holloway RL, Broadfield DC, Braun AR. 1998. Asymmetry of chimpanzee planum temporale: humanlike pattern of Wernicke's brain language area homolog. Science. 279: 220-222.

Garel C, Chantrel E, Brisse H, Elmaleh M, Luton D, Oury JF *et al.* 2001. Fetal cerebral cortex: normal gestational landmarks identified using prenatal MR imaging. AJNR Am J Neuroradiol. 22: 184-189.

Germanaud D, Lefevre J, Toro R, Fischer C, Dubois J, Hertz-Pannier L *et al.* 2012. Larger is twistier: spectral analysis of gyrification (SPANGY) applied to adult brain size polymorphism. Neuroimage. 63: 1257-1272.

Girard N, Raybaud C, Poncet M. 1995. In vivo MR study of brain maturation in normal fetuses. AJNR Am J Neuroradiol. 16: 407-413.

Glasel H, Leroy F, Dubois J, Hertz-Pannier L, Mangin JF, Dehaene-Lambertz G. 2011. A robust cerebral asymmetry in the infant brain: the rightward superior temporal sulcus. Neuroimage. 58: 716-723.

Habas PA, Scott JA, Roosta A, Rajagopalan V, Kim K, Rousseau F *et al.* 2012. Early folding patterns and asymmetries of the normal human brain detected from in utero MRI. Cereb Cortex. 22: 13-25.

Hill J, Dierker D, Neil J, Inder T, Knutsen A, Harwell J *et al.* 2010a. A surface-based analysis of hemispheric asymmetries and folding of cerebral cortex in term-born human infants. J Neurosci. 30: 2268-2276.

Hill J, Inder T, Neil J, Dierker D, Harwell J, Van ED. 2010b. Similar patterns of cortical expansion during human development and evolution. Proc Natl Acad Sci U S A. 107: 13135-13140.

Hopkins WD, Nir TM. 2010. Planum temporale surface area and grey matter asymmetries in chimpanzees (Pan troglodytes): the effect of handedness and comparison with findings in humans. Behav Brain Res. 208: 436-443.

Im K, Pienaar R, Lee JM, Seong JK, Choi YY, Lee KH *et al*. 2011. Quantitative comparison and analysis of sulcal patterns using sulcal graph matching: a twin study. Neuroimage. 57: 1077-1086.

Kapellou O, Counsell SJ, Kennea N, Dyet L, Saeed N, Stark J *et al*. 2006. Abnormal cortical development after premature birth shown by altered allometric scaling of brain growth. PLoS Med. 3: e265.

Kasprian G, Langs G, Brugger PC, Bittner M, Weber M, Arantes M *et al*. 2011. The prenatal origin of hemispheric asymmetry: an in utero neuroimaging study. Cereb Cortex. 21: 1076-1083.

Kaukola T, Kapellou O, Laroche S, Counsell SJ, Dyet LE, Allsop JM *et al*. 2009. Severity of perinatal illness and cerebral cortical growth in preterm infants. Acta Paediatr. 98: 990-995.

Kersbergen KJ, Leemans A, Groenendaal F, van der Aa NE, Viergever MA, de Vries LS *et al*. 2014. Microstructural brain development between 30 and 40 weeks corrected age in a longitudinal cohort of extremely preterm infants. Neuroimage. 103C: 214-224.

Kinney HC, Brody BA, Kloman AS, Gilles FH. 1988. Sequence of central nervous system myelination in human infancy. II. Patterns of myelination in autopsied infants. J Neuropathol Exp Neurol. 47: 217-234.

Lefevre J, Germanaud D, Dubois J, Rousseau F, de Macedo Santos I, Angleys H *et al*. 2015. Are developmental trajectories of cortical folding comparable between cross-sectional datasets of fetuses and preterm newborns? Cerebral Cortex doi: 10.1093/cercor/bhv123.

Leroy F, Cai Q, Bogart SL, Dubois J, Coulon O, Monzalvo K *et al*. 2015. New human-specific brain landmark: The depth asymmetry of superior temporal sulcus. Proc Natl Acad Sci U S A. pii: 201412389.

Leroy F, Mangin JF, Rousseau F, Glasel H, Hertz-Pannier L, Dubois J *et al*. 2011. Atlas-free surface reconstruction of the cortical grey-white interface in infants. PLoS One. 6: e27128.

Levene MI. 1981. Measurement of the growth of the lateral ventricles in preterm infants with real-time ultrasound. Arch Dis Child. 56: 900-904.

Li G, Nie J, Wang L, Shi F, Lyall AE, Lin W *et al*. 2014. Mapping longitudinal hemispheric structural asymmetries of the human cerebral cortex from birth to 2 years of age. Cereb Cortex. 24: 1289-1300.

Mahmoudzadeh M, Dehaene-Lambertz G, Fournier M, Kongolo G, Goudjil S, Dubois J *et al*. 2013. Syllabic discrimination in premature human infants prior to complete formation of cortical layers. Proc Natl Acad Sci U S A. 110: 4846-4851.

Mangin JF, Riviere D, Cachia A, Duchesnay E, Cointepas Y, Papadopoulos-Orfanos D *et al*. 2004. A framework to study the cortical folding patterns. Neuroimage. 23 Suppl 1: S129-S138.

Melbourne A, Kendall GS, Cardoso MJ, Gunny R, Robertson NJ, Marlow N *et al*. 2014. Preterm birth affects the developmental synergy between cortical folding and cortical connectivity observed on multimodal MRI. Neuroimage. 89: 23-34.

Moeskops P, Benders MJ, Chit SM, Kersbergen KJ, Groenendaal F, de Vries LS *et al*. 2015. Automatic segmentation of MR brain images of preterm infants using supervised classification. Neuroimage. 118: 628-641.

Moeskops P, Benders MJNL, Pearlman PC, Kersbergen KJ, Leemans A, Viergever MA *et al*. 2013. Assessment of quantitative cortical biomarkers in the developing brain of preterm infants. SPIE Medical Imaging vol. 8670.

Ochiai T, Grimault S, Scavarda D, Roch G, Hori T, Riviere D *et al*. 2004. Sulcal pattern and morphology of the superior temporal sulcus. Neuroimage. 22: 706-719.

Papile LA, Burstein J, Burstein R, Koffler H. 1978. Incidence and evolution of subependymal and intraventricular hemorrhage: a study of infants with birth weights less than 1,500 gm. J Pediatr. 92: 529-534.

Perrot M, Riviere D, Mangin JF. 2011. Cortical sulci recognition and spatial normalization. Med Image Anal. 15: 529-550.

Rathbone R, Counsell SJ, Kapellou O, Dyet L, Kennea N, Hajnal J *et al*. 2011. Perinatal cortical growth and childhood neurocognitive abilities. Neurology. 77: 1510-1517.

Smith SM. 2002. Fast robust automated brain extraction. Hum Brain Mapp. 17: 143-155.

Sowell ER, Thompson PM, Rex D, Kornsand D, Tessner KD, Jernigan TL *et al*. 2002. Mapping sulcal pattern asymmetry and local cortical surface gray matter distribution in vivo: maturation in perisylvian cortices. Cereb Cortex. 12: 17-26.

Tallinen T, Chung JY, Biggins JS, Mahadevan L. 2014. Gyrification from constrained cortical expansion. Proc Natl Acad Sci U S A. 111: 12667-12672.

Toro R, Burnod Y. 2005. A morphogenetic model for the development of cortical convolutions. Cereb Cortex. 15: 1900-1913.

van der Knaap MS, van Wezel-Meijler G, Barth PG, Barkhof F, Ader HJ, Valk J. 1996. Normal gyration and sulcation in preterm and term neonates: appearance on MR images. Radiology. 200: 389-396.

Van Essen DC. 1997. A tension-based theory of morphogenesis and compact wiring in the central nervous system. Nature. 385: 313-318.

Van Essen DC. 2005. A Population-Average, Landmark- and Surface-based (PALS) atlas of human cerebral cortex. Neuroimage. 28: 635-662.

Vasileiadis GT, Thompson RT, Han VK, Gelman N. 2009. Females follow a more "compact" early human brain development model than males. A case-control study of preterm neonates. Pediatr Res. 66: 551-555.

Visser GH, Eilers PH, Elferink-Stinkens PM, Merkus HM, Wit JM. 2009. New Dutch reference curves for birthweight by gestational age. Early Hum Dev. 85: 737-744.

Wright R, Kyriakopoulou V, Ledig C, Rutherford MA, Hajnal JV, Rueckert D *et al*. 2014. Automatic quantification of normal cortical folding patterns from fetal brain MRI. Neuroimage. 91: 21-32.

Xu G, Knutsen AK, Dikranian K, Kroenke CD, Bayly PV, Taber LA. 2010. Axons pull on the brain, but tension does not drive cortical folding. J Biomech Eng. 132: 071013.